

MHD Thermal Radiative Stretching Surface of a Micropolar Nanofluid Flow with Heat Source Parameter

Srinivas Maripala¹, Kishan Naikoti²

¹Department of mathematics, Sreenidhi Institute of Science and Technology, Ghatkesar, Hyderabad, Andhra Pradesh, India

²Department of Mathematics, Osmania University, Hyderabad, Andhra Pradesh, India

ABSTRACT

A numerical study of variable thermal conductivity and radiation on the flow and heat transfer of an electrically conducting micropolar nanofluid over a continuously stretching surface with varying temperature in the presence of a magnetic field and heat source/sink is presented. The governing conservation equations of Angular momentum, energy, momentum and mass are converted into a system of non-linear ordinary differential equations by means of similarity transformation. The resulting coupled system non-linear ordinary differential equations are solved by implicit finite difference method along with the Thomas algorithm. The results are analyzed for the effect of different physical parameters on velocity, angular velocity, temperature and concentration fields are presented through graphs.

Keywords : MHD, microrotation parameter, radiation parameter, thermal conductivity parameter, , heat source/sink.

I. INTRODUCTION

The nanofluid is changed with the thermal conductivity has attracted the interest of many scientists and researchers. The survey of convective heat transfer in nanofluid by Buongiorno[1]. He predicted that the nanoparticles' absolute velocity is roughly a sum of the slip velocity and base fluid velocity. He focused on fluid drainage, inertia, Brownian diffusion, thermophoresis, diffusiophoresis and the gravity setting as the effective quantities and concluded that for the laminar type flow, only the Brownian diffusion and the thermophoresis have noticeable effects. The influence of nanoparticles on a natural convection boundary layer flow passing a vertical plate has observed by the Kuznetsov and Nield[2]. They considered the nanoparticle fraction and temperature both to be constant along the wall and concluded that the reduced Nusselt number is a decreasing function of the nanofluid numbers. The onset of convection in a horizontal layer of a porous medium layer saturated by a nanofluid through the use of linear instability theory is examined by Nield and Kuznetsov[3] and the convection in a horizontal layer uniformly heated from the bottom, known as the Benard problem, was studied by Tzou.[4]. Furthermore, Eastman et al.[5] used pure copper nanoparticles of size

less than 10nm and achieved an increase of 40 in thermal conductivity for only 0.3 volume fraction of the solid dispersed in ethyleneglycal. The mixed boundary layer convection flow passing a vertical flat plate embedded in a porous medium filled with a nanofluid (the basic fluid was considered to be water was studied by Ahmad and Pop.[6]. The theory of thermomicropolar fluids was developed by Eringen [7] by extending his theory of micropolar fluid. The flow characteristics of the boundary layer of micropolar fluid over a semi-infinite plate in different situations have been studied by many authors. Recently, Srinivas Maripala and Kishan Naikoti[13] studied the MHD convection slip flow of a thermosolutal nanofluid in a saturated porous media over a radiating stretching sheet with heat source/sink.

II. METHODS AND MATERIAL

Consider a steady two-dimensional flow of an incompressible, electrically conducting micropolar nanofluid, subject to a transverse magnetic field over a semi-infinite stretching plate with variable temperature in the presence of radiation. The X-axis is directed along the continuous stretching plate and points in the direction of motion. The X-axis and Y-axis are

perpendicular to each other and to the direction of the slot (the Z-axis), so the continuous stretching plate issues. The induced magnetic field and the Joule heating are neglected is assumed. It is assumed that the fluid properties are constant, except for the fluid thermal

conductivity which is taken as a linear function of temperature profiles. Then the governing equations under the usual boundary layer approximations for the problem can be written as follows [8]:

$$\frac{\partial \bar{u}}{\partial x} + \frac{\partial \bar{v}}{\partial y} = 0 \quad (1)$$

$$\bar{u} \frac{\partial \bar{u}}{\partial x} + \bar{v} \frac{\partial \bar{u}}{\partial y} = \bar{v} \frac{\partial^2 \bar{u}}{\partial y^2} + K_1 \frac{\partial \sigma}{\partial y} - \frac{\sigma B_0^2}{\rho} \bar{u} \quad (2)$$

$$G_1 \frac{\partial^2 \sigma}{\partial y^2} - 2\sigma - \frac{\partial \bar{u}}{\partial y} = 0 \quad (3)$$

$$\rho c_p \left(\bar{u} \frac{\partial T}{\partial x} + \bar{v} \frac{\partial T}{\partial y} \right) = \frac{\partial}{\partial y} \left(k \frac{\partial T}{\partial y} \right) + \mu \left(\frac{\partial \bar{u}}{\partial y} \right)^2 - \frac{\partial q_r}{\partial y} + \tau \left[D_B \frac{\partial C}{\partial y} \frac{\partial T}{\partial y} + \frac{D_T}{T_\infty} \left(\frac{\partial T}{\partial y} \right)^2 \right] + \frac{Q_0}{(\rho c)_f} (T - T_\infty) \quad (4)$$

$$\frac{\partial C}{\partial t} + \bar{u} \frac{\partial C}{\partial x} + \bar{v} \frac{\partial C}{\partial y} = D_B \frac{\partial^2 C}{\partial y^2} + \frac{D_T}{T_\infty} \frac{\partial^2 T}{\partial y^2} \quad (5)$$

where $\bar{v} = (\mu + S)/\rho$ is the apparent kinematic viscosity, μ is the coefficient of dynamic viscosity, S is a constant characteristic of the fluid, σ is the microrotation component, $K_1 = S/\rho (> 0)$ is the coupling constant, $G_1 (> 0)$ is the microrotation constant, ρ is the fluid density, u and v are the components of velocity along x and y direction, respectively. T is the temperature of the fluid in the boundary layer, T_∞ is the temperature of the fluid far away from the plate, T_w is the temperature of the plate, k is the thermal conductivity, c_p is the specific heat at constant pressure, σ_0 is the electric conductivity, B_0 is an external magnetic field and q_r is the radiative heat flux. T is the temperature, C is the concentration of the fluid, C_p is the specific heat, q_r is the radiative heat flux, T_w and C_w - the temperature and concentration of the sheet, T_∞ and C_∞ - the ambient temperature and concentration, D_B - the Brownian diffusion coefficient, D_T the thermophoresis coefficient, Q_0 volumetric rate of heat generation/absorption, B_0 - the magnetic induction, $(\rho C)_p$ - the heat capacitance of the nanoparticles, $(\rho C)_f$ - the heat capacitance of the base fluid, and $\tau = (\rho C)_p/(\rho C)_f$ is the ratio between the effective heat capacity of the nanoparticles material and heat capacity of the fluid. And the boundary conditions of the problem are given by

components of velocity along x and y direction, respectively. T is the temperature of the fluid in the boundary layer, T_∞ is the temperature of the fluid far away from the plate, T_w is the temperature of the plate, k is the thermal conductivity, c_p is the specific heat at constant pressure, σ_0 is the electric conductivity, B_0 is an external magnetic field and q_r is the radiative heat flux. T is the temperature, C is the concentration of the fluid, C_p is the specific heat, q_r is the radiative heat flux, T_w and C_w - the temperature and concentration of the sheet, T_∞ and C_∞ - the ambient temperature and concentration, D_B - the Brownian diffusion coefficient, D_T the thermophoresis coefficient, Q_0 volumetric rate of heat generation/absorption, B_0 - the magnetic induction, $(\rho C)_p$ - the heat capacitance of the nanoparticles, $(\rho C)_f$ - the heat capacitance of the base fluid, and $\tau = (\rho C)_p/(\rho C)_f$ is the ratio between the effective heat capacity of the nanoparticles material and heat capacity of the fluid. And the boundary conditions of the problem are given by

$$\begin{aligned} y = 0, \quad \bar{u} = \alpha x, \quad \bar{v} = 0, \quad T = T_w(x), \quad \sigma = 0 \\ y \rightarrow \infty, \quad \bar{u} \rightarrow 0, \quad T \rightarrow T_\infty, \quad \sigma \rightarrow 0 \end{aligned} \quad (6)$$

where $\bar{v} = (\mu + S)/\rho$ is the apparent kinematic viscosity, μ is the coefficient of dynamic viscosity, S is a constant characteristic of the fluid, σ is the microrotation component, $K_1 = S/\rho (> 0)$ is the coupling constant, $G_1 (> 0)$ is the microrotation constant, ρ is the fluid density, u and v are the

The wall temperature is assumed to vary along the plate. According to the following power-law $T_w - T_\infty = \beta x^\gamma$, where β and γ (the surface temperature parameter) are constants. (7)

The fluid thermal conductivity is assumed to vary as a linear function of the temperature in the form [9]

$$k = k_{\infty} [1 + b(T - T_{\infty})] \quad (8)$$

where k_{∞} is the ambient thermal conductivity and b is a constant depending on the nature of the fluid. In general, $b > 0$ for air and liquids such as water, while $b < 0$ for fluids such as lubrication oils. Using Rosselant approximation [10] there is

$$q_r = (-4\sigma^*/3k^*) \frac{\partial T^4}{\partial y} \quad (9)$$

where σ^* is the Stefan Boltzmann constant and k^* is the mean absorption coefficient. In this study, we consider the case where the temperature differences within the flow are sufficiently small. Expanding T^4 in a Taylor series about T_{∞} and neglecting higher order terms [8], we have

$$T^4 \cong 4T_{\infty}^3 T - 3T_{\infty}^4 \quad (10)$$

Using Eq.(8), Eq.(4) becomes

$$\rho c_p \left(\bar{u} \frac{\partial T}{\partial x} + \bar{v} \frac{\partial T}{\partial y} \right) = \frac{\partial}{\partial y} \left(k \frac{\partial T}{\partial y} \right) + \mu \left(\frac{\partial \bar{u}}{\partial y} \right)^2 + \frac{16\sigma^* T_{\infty}^3}{3k^*} \frac{\partial^2 T}{\partial y^2} + \tau \left[D_B \frac{\partial C}{\partial y} \frac{\partial T}{\partial y} + \frac{D_T}{T_{\infty}} \left(\frac{\partial T}{\partial y} \right)^2 \right] + Q\theta \quad (11)$$

by using the following similarity transformations

$$\begin{aligned} \eta &= (\alpha/v)^{\frac{1}{2}} y, \quad \psi = (\alpha v)^{\frac{1}{2}} x f(\eta), \\ \bar{u} &= \frac{\partial \psi}{\partial y}, \quad \bar{v} = -\frac{\partial \psi}{\partial x}, \quad \sigma = (\alpha^3/v)^{1/2} x g(\eta), \\ \theta(\eta) &= \frac{T - T_{\infty}}{T_w - T_{\infty}}, \quad k = k_{\infty}(1 + S\theta) \end{aligned} \quad (12)$$

Substituting from Eq.(12) into Eqs.(1)-(3) and (10), we have

$$f''' + ff'' - f'^2 + G_1 g' - Mf' = 0 \quad (13)$$

$$G g'' - (2g + f'') = 0 \quad (14)$$

$$[4 + 3F(1 + S\theta)]\theta'' + 3FPr[f\theta' - \gamma f'\theta + Ec(f'')^2 + 3FS(\theta'')^2 + Pr[Nb\theta'\varphi' + Nt\theta'^2] + Q\theta = 0 \quad (15)$$

$$\varphi'' - Le f\varphi' + \frac{Nt}{Nb}\theta'' = 0 \quad (16)$$

Where

$M = (\sigma_0 B_0^2)/\rho\alpha$ (magnetic parameter),

$G_1 = K_1/v$ (coupling constant),

$Pr = (\mu c_p)/k_{\infty}$ (Prandtl number

$G = G_1 \alpha/v$ (microrotation parameter),)

$F = (k_{\infty} k^*)/(4\sigma^* T_{\infty}^3)$ (Radiation parameter),

$Ec = \frac{\alpha^2 x^2}{c_p(T_w - T_{\infty})}$ (Eckert number),

$S = b(T_w - T_{\infty})$ (thermal conductivity parameter),

$Nb = \tau D_B(C_w - C_{\infty})/v$ (Brownian motion parameter), $Nt = \tau D_T(T_w - T_{\infty})/vT_{\infty}$

(Thermophoresis parameter),

$Le = v/D_B$ (Lewies number),

γ = Surface temperature parameter

For air $0 \leq S \leq 6$, for water $0 \leq S \leq 0.12$ and for lubrication oils $-0.1 \leq S \leq 0$ [11]

The transformed boundary conditions are given by

$$\begin{aligned} f(0) &= 0, \quad f'(0) = 1, \quad \theta(0) = 1, \quad g(0) = 0, \\ f'(\infty) &= 0, \quad \theta(\infty) = 0, \quad g(\infty) = 0 \end{aligned} \quad (17)$$

From the velocity field we can study the wall shear stress, τ_w as given by [12]:

$$\tau_w = -\left| (\mu + S) \frac{du}{dy} + S\sigma \right| \text{ at } y = 0 \quad (18)$$

$$c_f = \left(\frac{2\tau}{\rho u^2} \right)_{y=0} = -2R_{ex}^{-1/2} f''(0) \text{ (skin friction coefficient)} \quad (19)$$

where $R_{ex} = \alpha x/v$ is the local Reynolds number. Eq. (20) shows the skin friction coefficient does not contain the microrotation term in an explicitly way.

$$q_w = -k \left(\frac{\partial T}{\partial y} \right) \text{ at } y = 0 \quad (\text{rate of heat transfer}) \quad (20)$$

$$h(x) = q_w / T_w - T_\infty \quad (\text{local heat transfer coefficient}) \quad (21)$$

$$N_{ux} = \frac{hx}{k} = -R_{ex}^{\frac{1}{2}} \theta'(0) \quad (\text{local Nusselt number}) \quad (22)$$

$$m_w = G_1 \left(\frac{\partial \sigma}{\partial y} \right)_{y=0} = R_{ex} \left(\frac{G_1 \alpha}{x} \right) g'(0) \quad (\text{couple stress}) \quad (23)$$

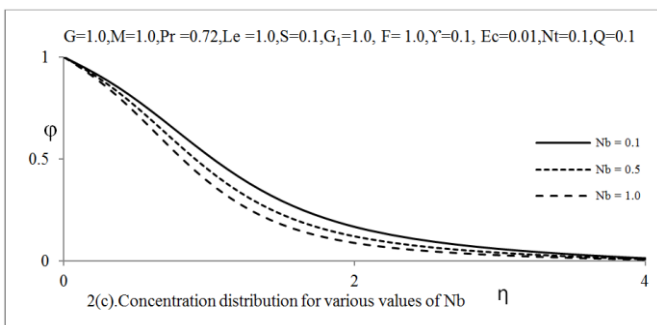
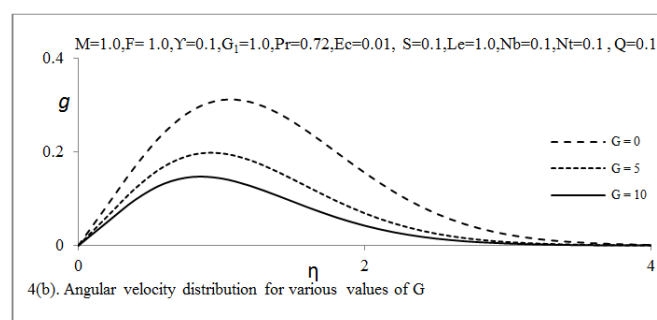
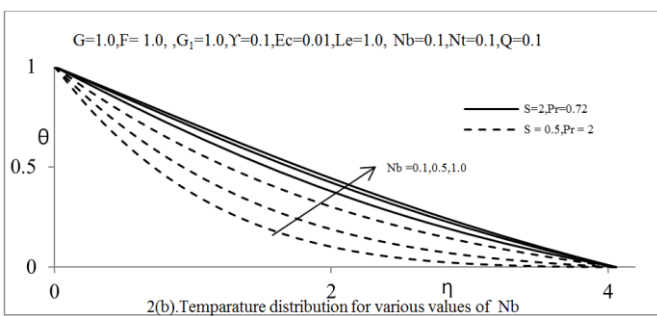
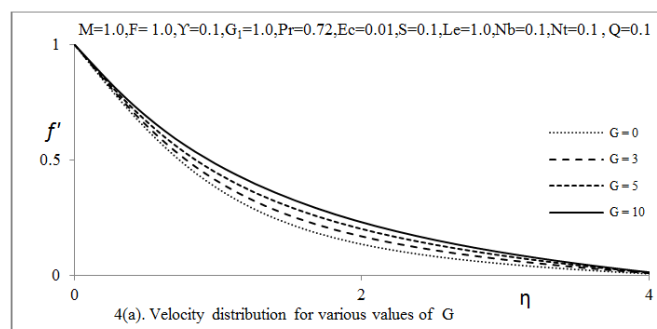
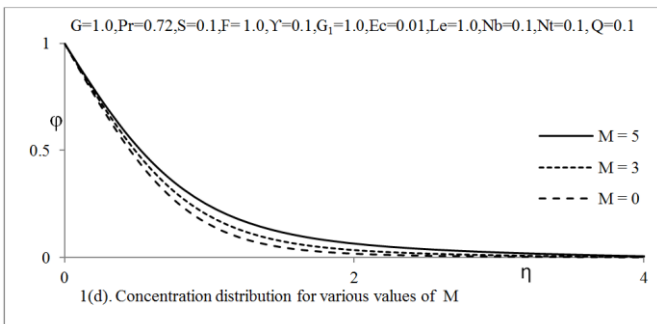
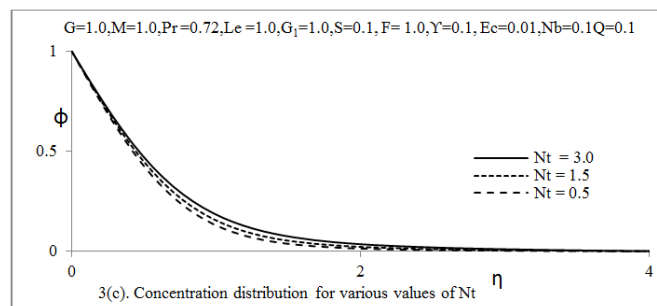
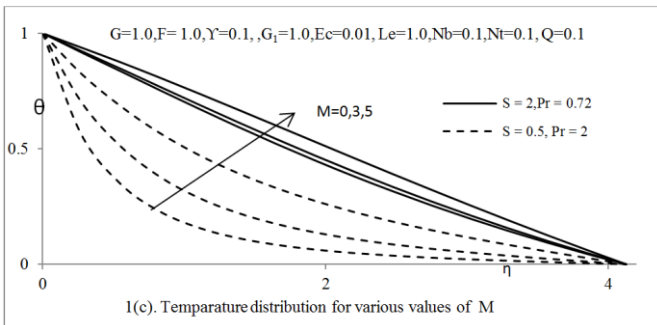
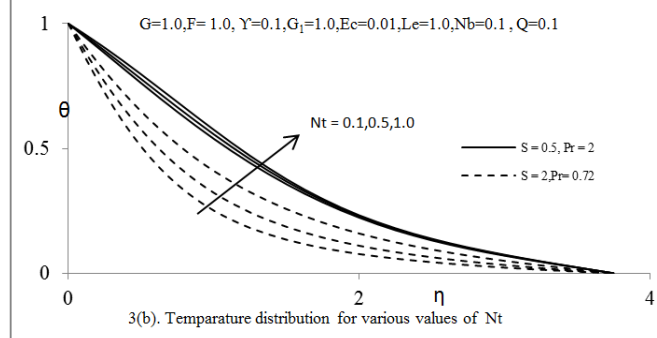
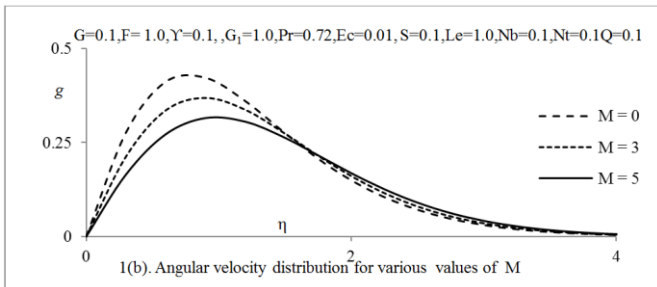
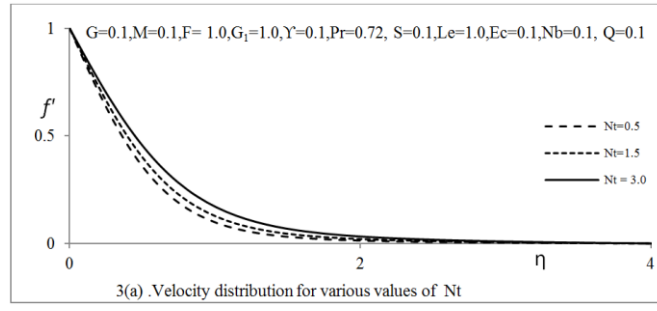
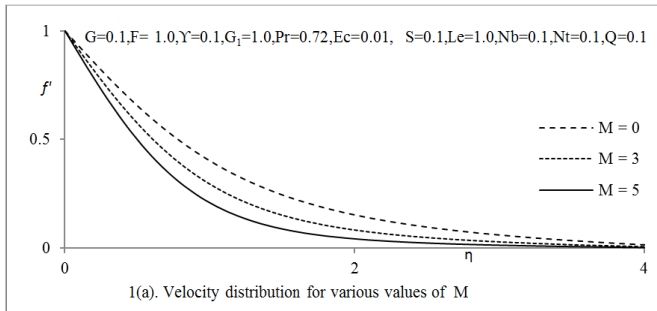
III. RESULTS AND DISCUSSION

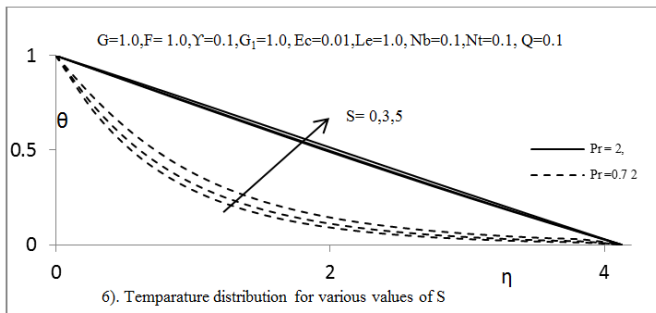
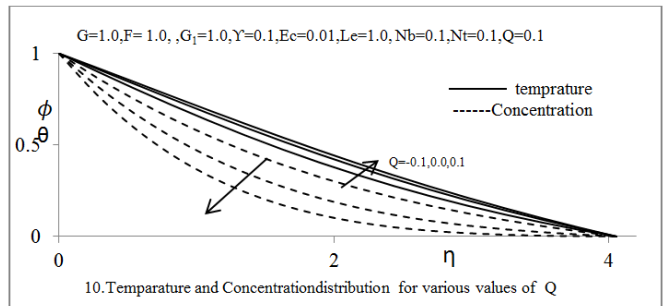
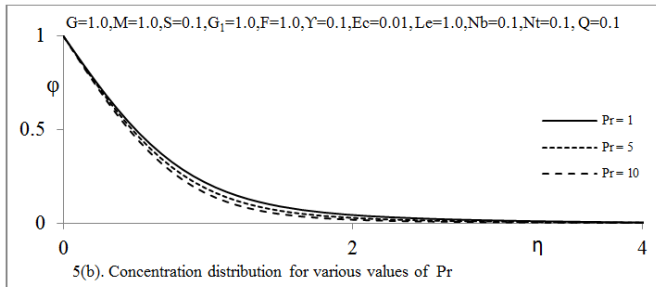
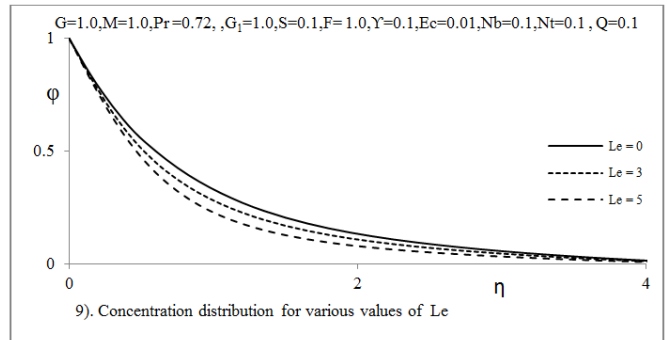
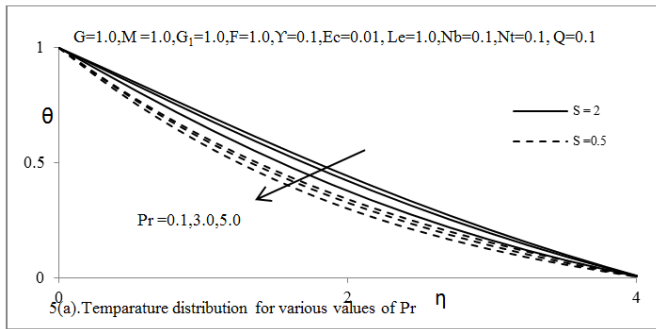
In order to solve the non-linear coupled equations (13) – (16) along with boundary conditions (17) an implicit finite difference scheme of Crank-Nicklson type has been employed. The computations have been carried out for various flow parameters on the velocity, angular velocity, temperature and concentration fields are presented through graphs. Figure 1(a)-1(d), it is observed that an increase in magnetic parameter M leads to a decrease in velocity profiles and angular velocity. The velocity boundary layer thickness becomes thinner as M increases. The thermal boundary layer thickness increases with increasing the magnetic parameter M is shown in figure 1(c). The reason for this behavior is that the Lorentz force increases the temperature. The concentration profiles are increased with the increase of magnetic field parameter M , is observed from Figure 1(d). The effect of Brownian motion parameter N_b on velocity, temperature and concentration profiles are shown in figures 2(a) - 2(c). The velocity profiles are decreased with the increase of Brownian motion parameter N_b . Figure 2(b), illustrates that the temperature profiles are increased as Brownian motion parameter N_b increases. Figure 2(c) depict that Concentration profiles are decreased, when Brownian motion parameter N_b increases.

Figures 3(a)-3(c) present typical profile for temperature and concentration for various values of thermophoretic parameter N_t . It is observed that an increase in the thermophoretic parameter leads to

increase in fluid temperature and nanoparticle concentrations. The microrotation parameter G affects are explained in figures 4(a) and 4(b). Velocity and angular velocity distribution profiles are increased when microrotation parameter G increases. Figures 5(a) and 5(b) depict temperature profile θ and concentration profile ϕ , for different values of Prandtl number Pr . One can find that temperature of nanofluid particles decreases with the increase in Pr for both the cases $S=2$ and $S=0.5$, which implies viscous boundary layer is thicker than the thermal boundary layer and the reverse phenomenon is observed from Figure 5(b). That is the concentration profiles are decreased as Prandtl number Pr increases. Fig. 6 shows the effect of the thermal conductivity parameter S on the temperature. From this figure it is noticed that the temperature decreases with the increasing of S . The variation of the temperature θ with respect to η for different values of F is plotted and shown in Fig.7. From Fig.7 one sees that the temperature decreases with θ increasing the radiation parameter F . The reason of this trend can be explained as follows. The effect of radiation is to decrease the rate of energy transport to the fluid, thereby decreasing the temperature of the fluid. Fig.8 illustrates the effect of the surface temperature parameter γ on the temperature distribution θ . From Fig.8, It is observed that the temperature decreases as γ increases. Lewies number Le effects are seen in Figure9, that is the Lewies number Le , decreases the concentration profiles when it increases. Figures 10 illustrate the temperature and concentration profiles for different values of heat source/sink parameter Q . From figure 10, it reveal that with the effect of heat source/sink parameter ($Q < 0$), the temperature profiles decreases and the temperature profiles increase with heat source ($Q > 0$) and the effect of heat source/sink parameter Q , on concentration profiles. The concentration profiles increase in case of heat source/sink $Q < 0$, while the concentration profiles decreases with heat source/sink parameter $Q > 0$.

Graphs

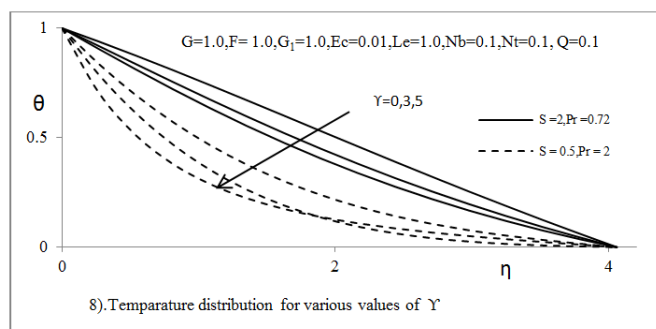
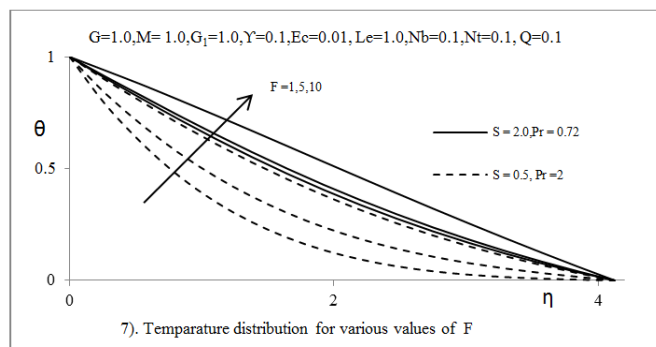




Physical quantities such as skin friction coefficient $f''(0)$, the couple stress coefficient $-g'(0)$, local nusselt number $\theta'(0)$, and Sherwood parameter $\phi'(0)$ are also computed and are shown in table. It is evident that with the increase of magnetic parameter M , radiation parameter F , surface temperature γ and thermal radiative parameter S , increases skin friction coefficient $f''(0)$, and couple stress coefficient $-g'(0)$, decreases the local nusselt number $\theta'(0)$ and Sherwood parameter $\phi'(0)$.

IV. CONCLUSION

In this paper, an analysis is presented the effects of variable thermal conductivity and radiation on the flow and heat transfer of an electrically conducting micropolar nanofluid over a continuously stretching surface with varying temperature in the presence of a magnetic field and heat source/sink. The governing conservation equations of mass, momentum, angular momentum and energy are converted into a system of non-linear ordinary differential equations by means of similarity transformation. The resulting system of coupled non-linear ordinary differential equations is solved by implicit finite difference method. The results are analyzed for the effect of different physical parameters such as magnetic parameter, Prandtl number, Eckert number, thermal conductivity parameter, heat source/sink, Lewies number, surface temperature parameter on the velocity, angular velocity, temperature and concentration fields are presented through graphs.



V. REFERENCES

- [1]. Buongiorno J 2006 ASME J. Heat Transfer 128 240
- [2]. Kuznetsov A V and Nield D A 2010 Int. J. Theor. Sci. 49 243
- [3]. Nield D A and Kuznetsov A V 2009 Int. J. Heat Mass Transfer 52 5796
- [4]. Tzou D Y 2008 ASME J. Heat Transfer 130 72401.
- [5]. Eastman J A, Choi S U S, Li S, Yu W and Thompson L J 2001 Appl. Phys. Lett. 78 718
- [6]. Ahmad S and Pop I 2010 Int. Commun. Heat Mass Transfer 37 987
- [7]. A.C. Eringen, Theory of thermomicro fluids, Math. Anal. 38 (1972) 480–496.
- [8]. A. Raptis, Flow of a micropolar fluid past a continuously moving plate by the presence of radiation, Int. J. Heat Mass Transfer 41(1998) 2865–2866.
- [9]. J.C. Slattery, Momentum, Energy and Mass Transfer in Continua, McGraw-Hill, New York, 1972.
- [10]. E.M. Sparrow, R.D. Cess, Radiation Heat Transfer, Hemisphere Publishing Corporation, Washington, DC, 1978.
- [11]. H. Schlichting, Boundary Layer Theory, McGraw-Hill, New York, 1968.
- [12]. V.M. Soundalgekar, H.S. Takhar, Flow of micropolar fluid past a continuously moving plate, Int. J. Eng. Sci. 21 (1983) 961–965.
- [13]. Srinivas Maripala and Kishan Naikoti, MHD effects on micropolar nanofluid flow over a radiative stretching surface with thermal conductivity, Advances in Applied Science Research, 2016, 7(3):73-82.
- [14]. Srinivas Maripala and Kishan Naikoti, MHD convection slip flow of a thermosolutal nanofluid in a saturated porous media over a radiating stretching sheet with heat source/sink, Advances and Applications in Fluid Mechanics 18 (2), 177.